

# QuikSCAT Geophysical Model Function for Tropical Cyclones and Application to Hurricane Floyd

Simon H. Yueh, *Member, IEEE*, Bryan W. Stiles, *Member, IEEE*, Wu-Yang Tsai, Hua Hu, and W. Timothy Liu

**Abstract**—The QuikSCAT radar measurements of several tropical cyclones in 1999 have been studied to develop the geophysical model function (GMF) of Ku-band radar  $\sigma_0$ s for extreme high wind conditions. To account for the effects of precipitation, we analyze the co-located rain rates from the Special Sensor Microwave/Imager (SSM/I) and propose the rain rate as a parameter of the GMF. The analysis indicates the deficiency of the NSCAT2 GMF developed for the NASA scatterometer, which overestimates the ocean  $\sigma_0$  for tropical cyclones and ignores the influence of rain. It is suggested that the QuikSCAT  $\sigma_0$  is sensitive to the wind speed of up to about  $40\text{--}50\text{ m}\cdot\text{s}^{-1}$ . We introduce modifications to the NSCAT2 GMF and apply the modified GMF to the QuikSCAT observations of Hurricane Floyd. The QuikSCAT wind estimates for Hurricane Floyd in 1999 was improved with the maximum wind speed reaching above 60 m/s. We perform an error analysis by comparing the QuikSCAT winds with the analyses fields from the National Oceanic and Atmospheric Administration (NOAA) Hurricane Research Division (HRD). The reasonable agreement between the improved QuikSCAT winds and the HRD analyses supports the applications of scatterometer wind retrievals for hurricanes.

**Index Terms**—Radar, remote sensing, sea surface, wind.

## I. INTRODUCTION

**S**KILLFUL forecasts of the tropical cyclone (TC) track and intensity depend on a proper depiction of the initial air and sea states in TC forecast models [1]. A primary source of difficulty in past efforts for TC forecasting has been the inability to make direct observations of the surface wind field, which is one of the key driving forces for the heat and moisture exchange between the air and sea surfaces [5], [11], [12], [14].

The spaceborne scatterometers, designed to measure ocean surface winds, have a potential to provide the needed data set for hurricane monitoring and research. Scatterometers are a microwave radar specifically designed to make high precision measurements of the normalized radar cross section ( $\sigma_0$ ) of ocean surfaces. Because of the sensitivity of  $\sigma_0$  to ocean surface roughness, which is influenced by the surface wind velocity, it is feasible to estimate the ocean surface wind velocity from microwave scatterometer observations. The NASA satellite scatterometers operating at Ku-band frequency ( $\sim 13$  GHz), including the NASA scatterometer (NSCAT) onboard the

Japanese Advanced Earth Observation Satellite (ADEOS-1) from September 1996 to June 1997 [15] and the first NASA SeaWinds scatterometer on the QuikSCAT spacecraft [8] operating since June 1999 have been launched for the measurement of ocean surface wind fields. The second NASA SeaWinds scatterometer together with the Japanese Advanced Microwave Scanning Radiometer (AMSR) is planned for launch on the ADEOS-2 in November 20012.

The relationship between the ocean  $\sigma_0$  and the surface wind velocity is usually described by a geophysical model function (GMF). An approach for deriving the scatterometer GMF for ocean surfaces is to empirically correlate the radar measurements with the numerical weather model wind fields [7], [23] and has been utilized to obtain the NSCAT2 model function [24] for the NASA scatterometers. This approach appears effective for light and moderate winds, but the resulting GMFs for high winds ( $> 20$  m/s) are inaccurate due to the problematic accuracy of numerical wind analyses for high winds [13].

Similar deficiency is present in the wind estimates from the European Earth Remote Sensing Satellite (ERS-1 and -2) scatterometers operating at C-band (5.3 GHz) frequency. Several ERS-1 scatterometer passes of the Western Pacific TCs [21] suggest that the ERS scatterometer computed maximum wind speeds are lower than expected by about  $20\text{--}40\text{ m}\cdot\text{s}^{-1}$ . It has been postulated by [21] that three major error sources are limiting the high wind measurement performance of spaceborne scatterometers:

- 1) deficiencies of the geophysical model function for high winds;
- 2) effects of rain in terms of volume scattering from rain drops, rain-generated sea surface roughness [2], [3], and microwave attenuation of sea surface scattering;
- 3) wind gradient in the sensor footprint near the eyewall where the maximum wind speeds are expected.

To make a direct assessment of the ocean  $\sigma_0$ s for high winds, numerous aircraft scatterometer flights have been conducted over tropical cyclones. The aircraft experiment carried out by the University of Massachusetts, Amherst, using a vertically polarized scatterometer [4] demonstrated that there were wind speed signals in radar  $\sigma_0$ s of TCs. Further, vertically polarized radar measurements [6], [27] support the postulation by [21] that the NSCAT2 GMF overestimates the ocean  $\sigma_0$ . The dual-polarized observations [27] indicate that the Ku-band radar signature is polarized for hurricane conditions and the horizontal polarization is more sensitive to the wind speed than the vertical polarization. With these sets of aircraft data, modified model functions [13], [27] have been proposed, but there is still a systematic underestimate of wind speeds for above 30 m/s winds ([13,

Manuscript received June 12, 2001; revised August 7, 2001. This work was supported in part by the SeaWinds Scatterometer Project and the Jet Propulsion Laboratory, Pasadena, CA, under a contract with the National Aeronautics and Space Administration, Washington, DC.

The authors are with the Jet Propulsion Laboratory, California Institute of Technology, Pasadena, CA 91109 USA.

Publisher Item Identifier S 0196-2892(01)10244-5.

Figs. 12 and 15)). The effects of rain and wind gradient have apparently not yet been properly considered for the scatterometer wind retrievals.

We suggest that the first step toward developing the scatterometer wind retrieval algorithms for tropical cyclones is to improve our understanding of the relationship between the scatterometer  $\sigma_0$  and ocean wind speed for extreme high wind conditions. We have explored the effects of rain on the scatterometer  $\sigma_0$  measurements for high wind speeds ( $> 20$  m/s) through the analysis of QuikSCAT data, and the rain rate estimates from the passive microwave brightness temperatures acquired by the Special Sensor Microwave/Imager (SSM/I) deployed on the Defense Meteorological Satellite Program (DMSP) [10]. One objective is to determine whether the scatterometer  $\sigma_0$ s is sensitive to the wind speed for high winds, even under precipitating conditions. The other objective is to determine whether the effects of rain can be reduced by using the collocated scatterometer and radiometer data set for wind speed estimates.

Section II describes the observed dependence of QuikSCAT  $\sigma_0$  on wind speed and SSM/I rain rate for several hurricanes in 1999. An empirical relationship between the  $\sigma_0$  and the rain rate is derived. As a consistency check, we applied the empirical relationship to the QuikSCAT observations of Hurricane Floyd in 1999. We also examined the effects of wind gradient by processing the QuikSCAT/Floyd data at two gridded resolutions. The results are described in Section III. Section IV summarizes the results of our analysis and suggests areas for further studies.

## II. QUIKSCAT $\sigma_0$ FOR HIGH WIND SPEEDS

The SeaWinds scatterometer is a Ku-band (13.402 GHz) radar with a conical scanning antenna [8]. There are two feed horns illuminating a parabolic reflector to produce two antenna beams at  $46^\circ$  and  $54^\circ$  incidence angles on the earth surface. The inner antenna beam ( $46^\circ$  incidence) transmits and receives horizontal polarization, while the outer beam operates at vertical polarization. The antenna footprint size is about 30 km on the surface. A linear frequency-modulated chirp designed for the transmit pulse enables an improvement of the range resolution to about 5 km. The swath width of the inner beam is about 1400 km, comparable to that of SSM/I. The outer antenna beam provides a swath coverage of 1800 km, yielding more than 90% global coverage within a day.

To quantify the impact of rain on scatterometer observations, we examined the collocated QuikSCAT  $\sigma_0$  data and the rain rate estimates from three SSM/I instruments deployed on the DMSP satellites, F11, F13, and F14. The SSM/I rain retrievals, produced by Remote Sensing Systems [25], were registered to the QuikSCAT grids by Freilich and Vanhoff of the Oregon State University, Corvallis, for the QuikSCAT calibration and validation.

We examine the dependence of QuikSCAT  $\sigma_0$  on wind speed for tropical cyclones with an empirical approach. The QuikSCAT  $\sigma_0$ 's with the collocated SSM/I rain rate have been analyzed for 58 QuikSCAT passes of seven hurricanes in 1999 (Table I). The past difficulty of developing a scatterometer GMF for high winds was due to the lack of *in-situ* measurements that could be paired with the satellite microwave data. A technique

TABLE I  
THE NUMBER OF QUIKSCAT PASSES OVER THE PACIFIC AND ATLANTIC HURRICANES IN 1999 FOR THE ANALYSIS OF COLLOCATED QUIKSCAT AND SSM/I DATA

Name	Date	Location	Number of QuikSCAT Passes
Bret	August	Gulf of Mexico	3
Cindy	August	Atlantic	10
Dennis	August	Atlantic	12
Floyd	September	Atlantic	8
Gert	September	Atlantic	2
Eugene	August	Pacific	5
Dora	August	Pacific	18

proven effective by [26] used the wind fields from Holland's hurricane model [9] for the development of a high wind model function for GeoSat altimeter. This technique is similar to that described by [7], [24] with the numerical weather products for the development of a geophysical model function, except with a more accurate surface wind model for wind speeds above 30 m/s.

Following Young's approach, we applied Holland's model for the analysis of QuikSCAT data. It is recognized that Holland's model is a parametric model and is not expected to capture all the features of various hurricane wind fields. We considered our analysis as a first step toward understanding the feasibility of spaceborne scatterometers for the measurements of ocean surface winds for hurricanes. As will be shown, the results from our analysis justify our approach. Nevertheless, future work should consider the use of operational wind analyses for tropical cyclones, such as that from NOAA HRD, instead of Holland's model, for further improvement.

The gradient wind of Holland's model is expressed as

$$U_g = \left[ \frac{AB(p_n - p_0) \exp(-A/r^B)}{\rho r^B} + \frac{r^2 f^2}{4} \right]^{0.5} - \frac{rf}{2} \quad (1)$$

where

- $U_g$  gradient wind at radius  $r$  from the center of the storm;
- $\rho$  air density;
- $p_0$  central pressure;
- $p_n$  ambient pressure far from the storm;
- $f$  Coriolis parameter.

The parameters  $A$  and  $B$  are related to the radius of maximum wind ( $R_{\max}$ ) and the central pressure

$$A = R_{\max}^B \quad (2)$$

$$B = 1.5 + (980 - p_0)/120 \quad (3)$$

where  $p_0$  is expressed in millibars.  $R_{\max}$  and  $B$  define the size of the storm and the shape of the wind field.

We follow Young's description of the wind direction model [26] and derive the vector wind field from the gradient wind speed. It is assumed that the radial winds spiral in toward the storm with a constant inflow angle of  $25^\circ$  [26]. The 1-min averaged surface wind speed at 10 m height is obtained from the gradient wind speed by the application of a factor of 0.8 [16]. A forward motion vector  $\vec{V}_{fm}$  of the storm is added linearly to the azimuthally symmetric wind flow, resulting in an axially asymmetric wind field. We also rotate the maximum wind speed to

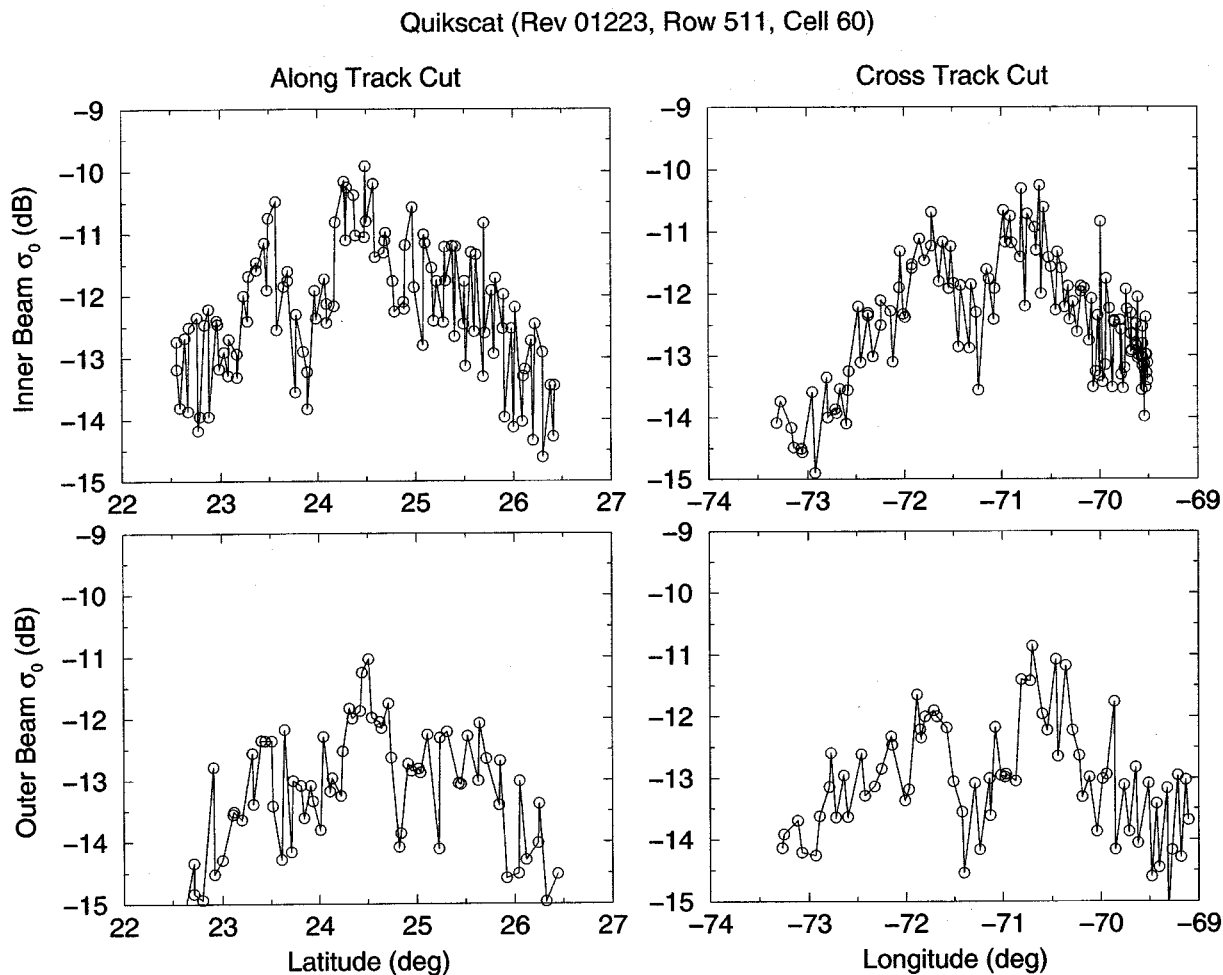


Fig. 1. QuikSCAT  $\sigma_0$ s along two cuts through the center of the Hurricane Floyd on September 13, 1999. The two left panels illustrate the  $\sigma_0$ s along the cut parallel to the spacecraft ground track, and the right panels illustrate the across-track cut. The center of the cyclone is located approximately at  $23.7^\circ$  latitude and  $-71.5^\circ$  longitude. The  $\sigma_0$ s from the inner antenna beam (horizontal polarization,  $46^\circ$  incidence) and the outer antenna beam (vertical polarization,  $55^\circ$  incidence) are plotted in the upper and lower panels, respectively. The data include both fore- and aft-look observations.

an angle of  $70^\circ$  to the direction of  $\vec{V}_{fm}$  (to the right in northern hemisphere and to the left in southern hemisphere) according to [22], [26]. An example of the wind field model is illustrated in [26].

The parameters of Holland's model include the location of the center, central pressure, radius of maximum wind and the velocity of forward motion. For our analysis, the ambient pressure is assumed to be 1000 mb. The only parameter not available from the National Hurricane Center (NHC) best track analysis is the radius of maximum wind, but it can be estimated from the scatterometer data in terms of the radius of maximum  $\sigma_0$  to the center. An example is given in Fig. 1, which illustrates the QuikSCAT  $\sigma_0$ s along two cuts through the center of Hurricane Floyd on September 13, 1999. The upper (lower) left panel indicates the  $\sigma_0$  from the QuikSCAT inner (outer) antenna beam along the cut parallel to the spacecraft ground track and the right panels indicate the data from the across track cut. The center of the cyclone is located approximately at  $23.7^\circ$  latitude and  $-71.5^\circ$  longitude, consistent with the NHC best track analysis. The  $\sigma_0$  peak is about  $-10.5$  dB located at about 40 km from the center and the  $\sigma_0$  decreases by about 3 dB along the cut to about

200 km off the center. We estimate the radius of maximum wind to be the distance from the center to the location of the maximum  $\sigma_0$ . Here we have neglected the effects of wind direction modulation on  $\sigma_0$ . This should not result in a significant error in the estimates of the radius of maximum wind because the direction of tangential wind does not vary dramatically along a radial cut near the eye.

The Holland's hurricane model is used to generate the surface wind velocity at the center of scatterometer footprint. The cyclones considered in our analysis are summarized in Table I. We obtain a total of about 47 000 QuikSCAT  $\sigma_0$  and SSM/I rain rate pairs for above 20 m/s wind speed with a 3-h time window. If the time window is reduced to 1 and 2 h of each QuikSCAT pass, the number of coreregistrations reduces to about 37 000 and 40 000, respectively. The QuikSCAT  $\sigma_0$ s are grouped into 4 m/s wind speed and 2 mm/h SSM/I rain rate bins. The average  $\sigma_0$  in each bin is illustrated as a function of wind speed for a range of rain rate in Fig. 2 for a QuikSCAT and SSM/I time difference of less than 2 h. Because the wind direction distribution of  $\sigma_0$ s in most bins is quite uniform and the wind direction modulation of  $\sigma_0$  appears quite small (less than 1–2 dB for above 30–40 m/s

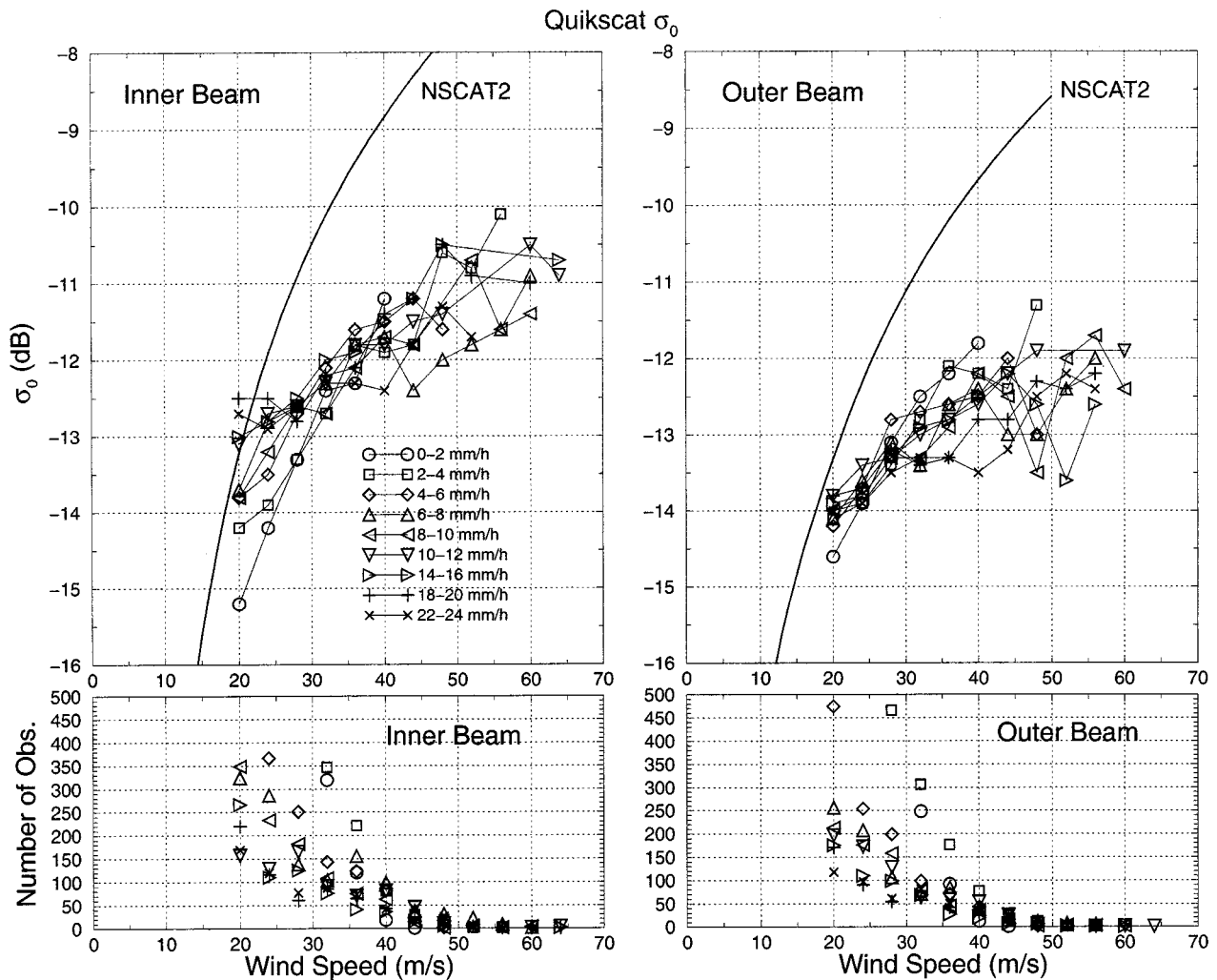


Fig. 2. Average QuikSCAT  $\sigma_0$  in dB versus wind speed for a range of collocated SSM/I rain rate. The QuikSCAT data were grouped into 4 m/s wind speed and 2 mm/h rain rate bins and the data in each bin were averaged. The upper left panel plots the data from the inner antenna beam operating at  $46^\circ$  incidence angle with horizontal polarization and the upper right panel plots the data from the outer antenna beam operating at  $54^\circ$  incidence angle with vertical polarization. Also included in each panel is the prediction by the NSCAT2 GMF. The two lower panels indicate the number of collocations in each bin.

wind speed), the residual wind direction effects in the average  $\sigma_0$  is expected to be much less than 1 dB. The total number of QuikSCAT-SSM/I pairs in each wind speed and rain rate bin, illustrated in the two lower panels, is about fifty to a few hundreds for 20–40 m/s wind speed and reduces with increasing wind speeds; therefore the average of the  $\sigma_0$  illustrated in the upper panels is more noisy for above 40 m/s wind speed.

Over the range of SSM/I rain rate ( $\leq 25$  mm/h), the QuikSCAT  $\sigma_0$  appears to increase with increasing wind speed of up to 40–50 m/s. The data are quite noisy for above 50 m/s wind speeds due to a limited number of collocations. For the lowest rain rate bin (0–2 mm/h), the QuikSCAT  $\sigma_0$ s from the inner beam increases by about 4 dB from 20 to 40 m/s, and those from the outer antenna beam change by about 3 dB. This is consistent with the aircraft scatterometer observations that the horizontally polarized  $\sigma_0$  has a larger wind speed sensitivity than the vertically polarized  $\sigma_0$  [27].

With an increase of rain rate, the wind speed sensitivity of QuikSCAT  $\sigma_0$  decreases, apparently due to an increase of volume scattering by rain drops, rain attenuation and scattering from rain roughened sea surfaces [2], [3]. The  $\sigma_0$  increases

with rain rate at 20 m/s, but has an opposite behavior at 40 m/s and above. Note that the curves corresponding to different rain rate in Fig. 2 cross each other at near 32 m/s for the inner beam data and at a lower wind speed of about 25 m/s for the outer beam data. This could be a result of the competition between the radar scattering from the rain drops and an attenuation of the surface scattering by rain: An increase in rain rate will increase the scattering from rain drops and rain-roughened water surfaces, but reduces the wind-induced surface scattering through attenuation. At near 20 m/s wind speed, rain drops have added substantial contributions to the radar scattering, but have not attenuated the wind-induced surface scattering by as much. The net effect is that the radar signal appears to increase with increasing rain rate at about 20 m/s wind speed. At above 40 m/s wind speeds, the wind-induced surface scattering appears to be stronger than the rain scattering and the rain-generated volume and surface scattering did not offset the reduction of wind-induced surface scattering through attenuation.

We have investigated the sensitivity of our results to the time difference between the QuikSCAT and SSM/I passes. Figs. 3 and 4 plot the average QuikSCAT  $\sigma_0$  for each bin versus the

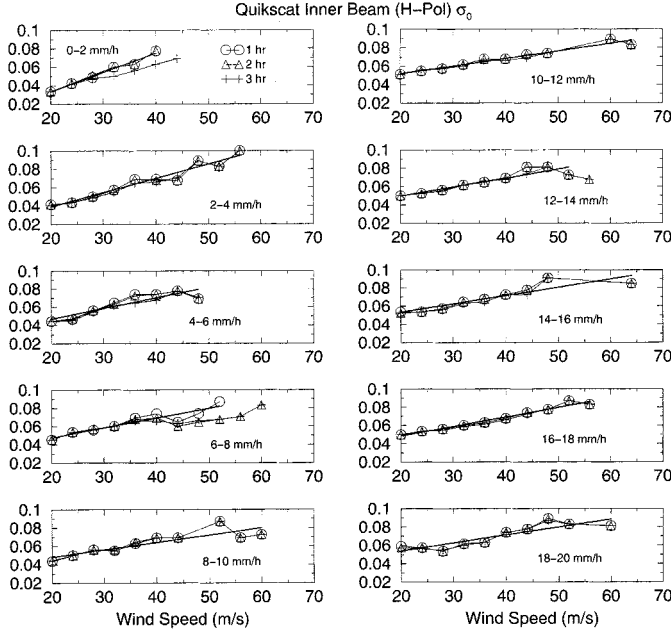


Fig. 3. Average QuikSCAT  $\sigma_0$  from the inner antenna beam versus wind speed for a range of collocated SSM/I rain rate. The QuikSCAT data were grouped into 4 m/s wind speed and 2 mm/h rain rate bins, and the data in each bin were averaged. Three curves were illustrated in each panel with 1-, 2- and 3-h thresholds for the time difference between QuikSCAT and SSM/I passes. The thick linear line represents the linear regression of the data with 1-h threshold.

wind speed for 1-, 2- and 3-h time windows. The changes are small when the time window is reduced from 3 to 2 h, and the results are essentially the same with 1- and 2-h thresholds.

Note that the  $\sigma_0$  is plotted in real number, instead of dB, in Figs. 3 and 4. There appears a quasilinear relationship between the QuikSCAT  $\sigma_0$  and wind speed in the range of 20–50 m/s wind speeds. The slope of the linear increasing trend is smaller for higher rain rate, which is expected from the effects of rain. The  $\sigma_0$  might have saturated and perhaps even decreased at above 50 m/s wind speed, but the limited number of observation for such extreme wind conditions prevent us from drawing a definitive conclusion.

The illustrations indicate that a linear wind-dependence model will be fairly accurate for QuikSCAT  $\sigma_0$  for up to about 50 m/s wind speed

$$\sigma_0 = \alpha + \beta(W - 20) \quad (4)$$

where  $\alpha$  and  $\beta$  are functions of rain rate. We estimate the coefficients with a linear regression model from the data for each rain rate bin plotted in Figs. 3 and 4. Fig. 5 illustrate  $\alpha$  (upper panels),  $\beta$  (middle panels) and the correlation coefficient of the linear regression model (lower panels) versus rain rate. The correlation coefficients are high, mostly above 0.8. We further fit  $\alpha$  and  $\beta$  with a quadratic polynomial

$$\alpha = \alpha_0 + \alpha_1 R + \alpha_2 R^2 \quad (5)$$

$$\beta = \beta_0 + \beta_1 R + \beta_2 R^2 \quad (6)$$

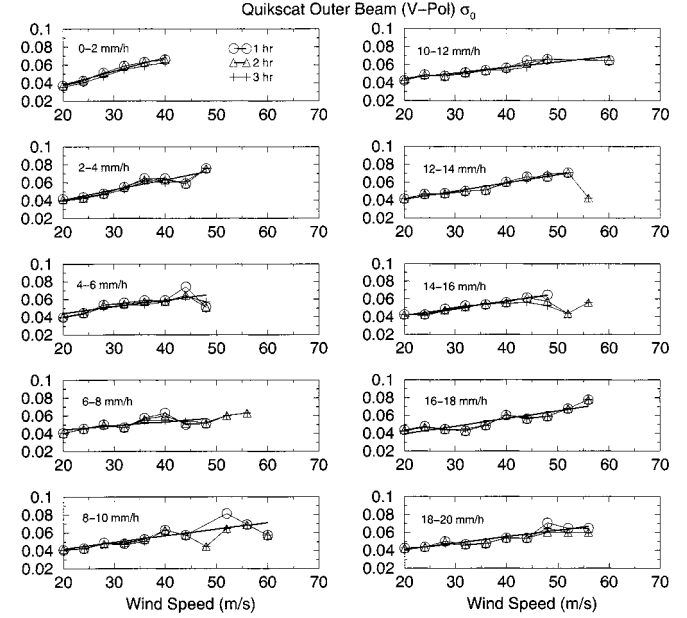


Fig. 4. Average QuikSCAT  $\sigma_0$  from the outer antenna beam versus wind speed for a range of collocated SSM/I rain rate. The QuikSCAT data were grouped into 4 m/s wind speed and 2 mm/h rain rate bins and the data in each bin were averaged. Three curves were illustrated in each panel with 1-, 2- and 3-h thresholds for the time difference between QuikSCAT and SSM/I passes. The thick linear line represents the linear regression of the data with 1-h threshold.

TABLE II  
QUADRATIC POLYNOMIAL EXPANSION COEFFICIENTS OF  $\alpha$  AND  $\beta$  AS A FUNCTION OF RAIN RATE FOR QUIKSCAT

Parameter	$\alpha_0, \beta_0$	$\alpha_1, \beta_1$	$\alpha_2, \beta_2$
Inner Beam $\alpha$	0.035	$2.35 \times 10^{-3}$	$-8.361 \times 10^{-5}$
Inner Beam $\beta$	0.00227	$-2.292 \times 10^{-4}$	$8.977 \times 10^{-6}$
Outer Beam $\alpha$	0.041	$7.82 \times 10^{-4}$	$-4.479 \times 10^{-5}$
Outer Beam $\beta$	0.0015	$-1.452 \times 10^{-4}$	$5.71 \times 10^{-6}$

where  $R$  is the SSM/I rain rate in mm/h. The coefficients are provided in Table II.

### III. QUIKSCAT WIND ESTIMATES FOR HURRICANE FLOYD

Although the QuikSCAT data indicate a wind speed sensitivity of the Ku-band radar  $\sigma_0$ s for hurricane winds, it remains to be shown on how well the wind speed can be retrieved from spaceborne scatterometer data for tropical cyclones. The data illustrated in Figs. 3 and 4 represent an ensemble average of the data over a variety of environmental conditions (Table I). Particularly, the precipitation associated with tropical storms typically has to be characterized by many parameters, including columnar height, vertical profile and rain drop size distribution, in addition to rain rate. If not taken into account, these parameters will introduce geophysical noise in the retrieval algorithm and hence errors in wind speed and direction estimates.

This section describes the application of an improved geophysical model function to Hurricane Floyd in 1999. We focus on Hurricane Floyd because we have obtained two analysis fields from the NOAA HRD for Hurricane Floyd, which will be used to evaluate the accuracy of the retrieval algorithm.

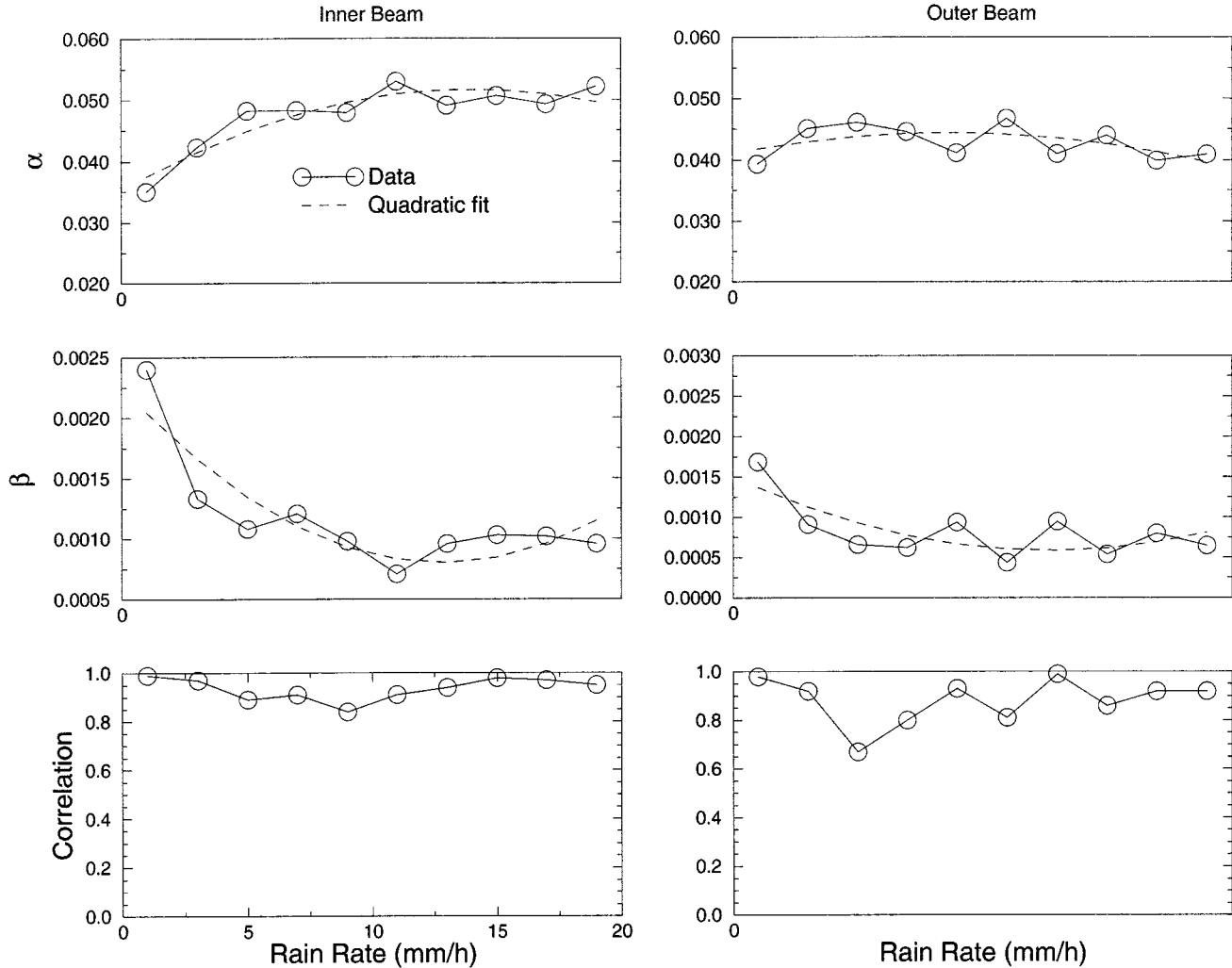


Fig. 5. Slopes and intercepts at 20 m/s wind speed of the linear  $\sigma_0$  regression model versus rain rate. The upper left panel plots for the QuikSCAT data from the inner antenna beam operating at horizontal polarization and the upper right panel plots the QuikSCAT data from the outer antenna beam operating at vertical polarization. The lower panels plot the correlation coefficients of the linear regression model, (4).

We modified the NSCAT2 GMF with the linear regression model (Table II) to retrieve the winds from the QuikSCAT measurements of hurricanes. The NSCAT2 GMF is expanded by a cosine series of wind direction  $\phi$

$$\sigma_0 = \sum_{n=0}^5 A_n \cos(n\phi) \quad (7)$$

where the coefficient  $A_n$  is a function of wind speed, incidence angle and polarization. We replace the  $A_0$  terms by the linear regression model (Table II) for wind speed above 20 m/s. It is known that the NSCAT2  $A_n$  coefficients also overestimate the wind direction modulation of  $\sigma_0$  [6], [27]. We use the empirical model described in [27] to adjust the  $A_n$  coefficients so that the ratio  $A_n/A_0$  is consistent with the aircraft observations. It is noticed that there is a discontinuity between the linear regression model and the NSCAT2 GMF at 20 m/s wind speed. To obtain a smooth transition, we linearly extrapolated the linear model to a lower wind speed where it meets the NSCAT2 GMF at about 15 m/s. The  $\sigma_0$  adjustment for 15–20 m/s wind speeds is about a few tenths of a dB. Because the NSCAT2 GMF is in tabular form, likewise the modified GMF, it is not possible to provide a closed-form representation.

The modified GMF, denoted as NSCAT-TC GMF, was used together with the collocated SSM/I rain rate to process the QuikSCAT data for the 1999 Hurricane Floyd. The QuikSCAT  $\sigma_0$  data were grouped into Wind Vector Cells (WVC) on a rectangular grid with a resolution of 25 km for QuikSCAT standard products. Under the assistance of the QuikSCAT Ground Processing System, one rev of QuikSCAT data over Hurricane Floyd on September 13, 1999 was gridded at a higher spatial resolution of 12.5 km, enabling us to investigate the effects of wind gradient. The data within each WVC contain the observations from antenna fore- and aft-look measurements. We used the maximum-likelihood estimator (MLE) implemented for the QuikSCAT ground data processing system to estimate the wind speed and direction from the gridded  $\sigma_0$ s. A simple modification is made to include the SSM/I rain rate as an additional input for the evaluation of model  $\sigma_0$ s for the MLE optimization

$$\text{MLE} = \sum_{i=1}^N \frac{[\sigma_{0i} - \sigma'_{0i}(W, \phi, R)]^2}{\text{var}(\sigma_{0i})} \quad (8)$$

where  $\sigma_{0i}$  is the radar measurement, and  $\sigma'_{0i}$  is from the model.

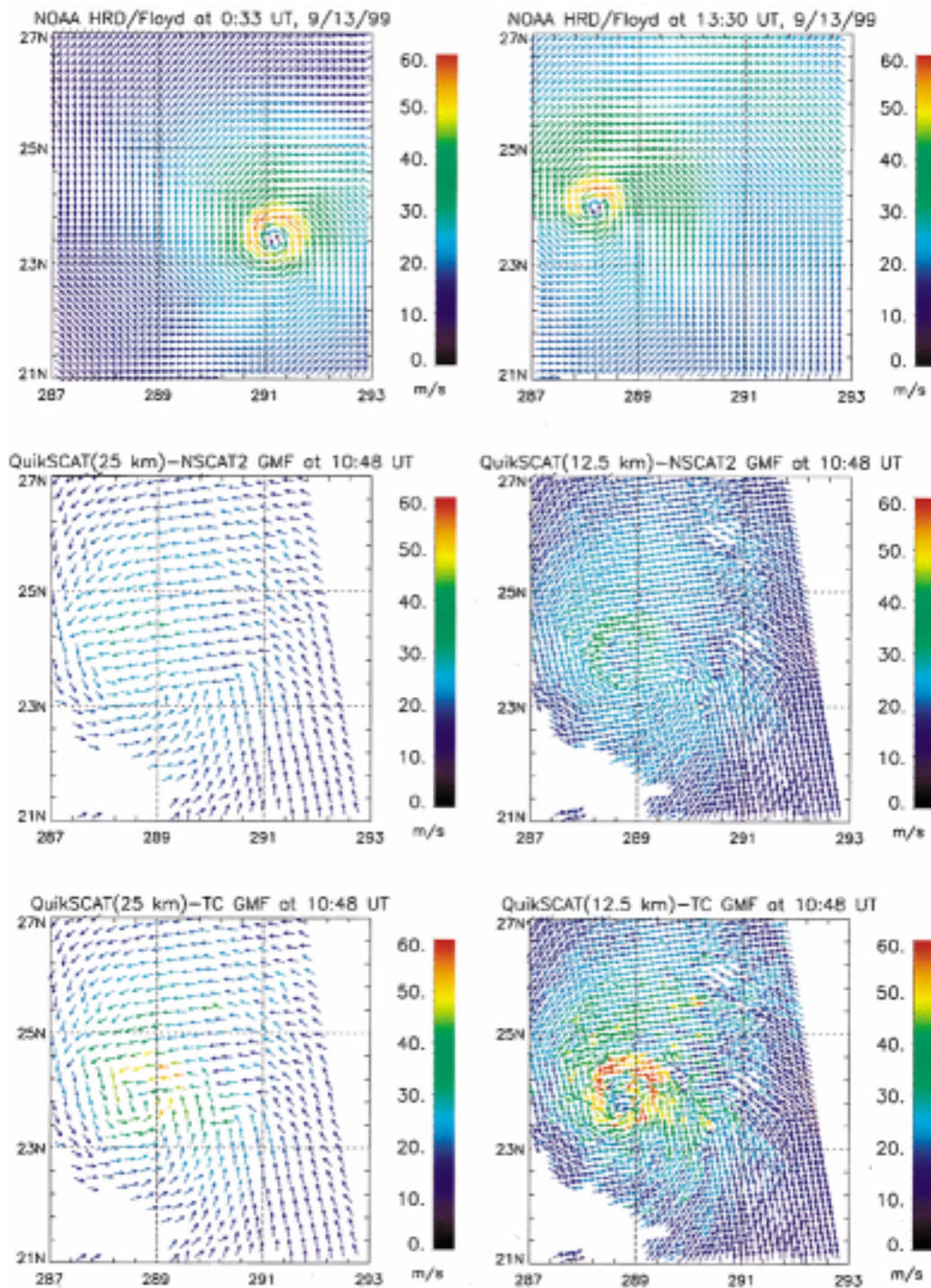


Fig. 6. NOAA HRD wind analyses and the QuikSCAT wind estimates for Hurricane Floyd on September 13, 1999. The HRD analyses are shown in the two upper panels. The QuikSCAT wind estimates from NSCAT2 GMF are plotted in the two middle panels, respectively, for 25 km and 12.5 km gridded resolution. The QuikSCAT winds estimated using the NSCAT-TC GMF and the SSM/I rain rate are plotted in the two lower panels for 25 km and 12.5 km resolution.

There are typically three to four local minima in the MLE, corresponding to multiple wind vector estimates (ambiguities) for each WVC. Depending on the noise level and structure, the global minimum may not be the closest to the actual wind direction. Following a procedure suggested by [13], we select the ambiguity with the direction closest to Holland's model wind field as the output. This procedure is not expected to be error-free, but should be effective in areas not far from the eyewall. This am-

biguity selection procedure is applied to the QuikSCAT observations of Hurricane Floyd with the NSCAT2 and NSCAT-TC model functions.

Hurricane Floyd on September 13, 1999 was a category four hurricane on the Saffir/Simpson Hurricane Scale with a maximum sustained wind speed of about 140 knots (70 m/s) according to the NHC best track analysis. QuikSCAT made a pass over Floyd at about 10:48 UT on September 13 when Floyd was

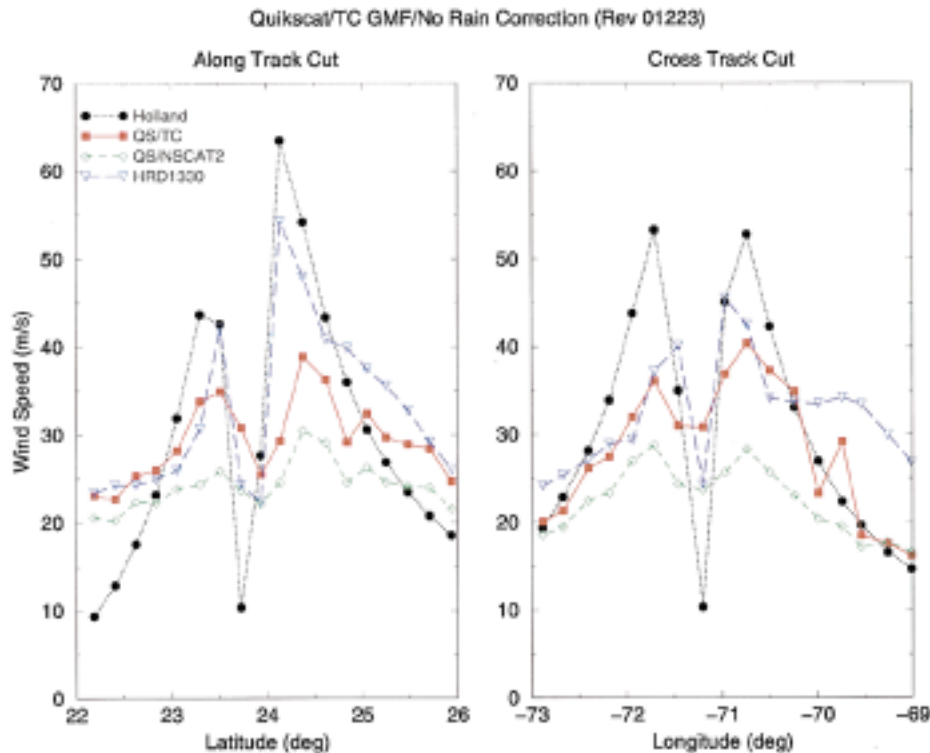


Fig. 7. Wind speed profiles of Hurricane Floyd on September 13, 1999. The left panel illustrates the along track cut through the center and the right panel illustrates the across-track cut. The wind vector cell resolution is 25 km. The QuikSCAT wind fields retrieved with the NSCAT2 (QS/NSCAT2) and the modified GMF without rain correction (QS/TC) are illustrated. The Holland's model wind and the HRD analyses at 13:30 UT are included for comparison.

at its maximum strength. The estimated QuikSCAT wind fields of Hurricane Floyd are illustrated together with the NOAA HRD analyses in Fig. 6. The two upper panels illustrate the NOAA HRD analyses at 0:33 UT and 13:30 UT. The NOAA HRD approach to hurricane wind analyses evolved from a series of studies of major landfalling hurricanes [17]–[19]. An HRD wind analysis requires the input of all available surface weather observations (e.g., ships, buoys, coastal platforms, surface aviation reports, reconnaissance aircraft data adjusted to the surface, etc.). Observational data are downloaded on a regular schedule and then processed to fit the analysis framework. This includes the data sent by NOAA P3 and G4 research aircraft during the HRD hurricane field program as well as U.S. Air Force Reserves C-130 reconnaissance aircraft, remotely sensed winds from the polar orbiting SSM/I and ERS satellite platforms and cloud drift winds derived from tracking low level visible cloud imagery from geostationary satellites. These data are composited relative to the storm over a 4–6 h period. All data are quality controlled and processed to conform to a common framework for height (10 m), exposure (marine or open terrain over land) and averaging period (maximum sustained 1 minute wind speed) using accepted methods from micrometeorology and wind engineering [18]. We notice that the maximum wind speed in the HRD analyses is about 60 m/s, which is about 10 m/s lower than the NHC best track analysis. The difference could represent the accuracy limitation of present techniques for specifying the strength of tropical cyclones.

The middle panels in Fig. 6 were the QuikSCAT wind retrievals from the NSCAT2 GMF at 25 km and 12.5 km gridded

processing resolution with the maximum wind speed in the range of 30–40 m/s, much lower than the intensity of Hurricane Floyd. The QuikSCAT wind estimates using the NSCAT-TC GMF illustrated in the two lower panels are in better agreement with the HRD analyses than the wind estimates with the NSCAT2 GMF.

The effects of rain are explored by processing the QuikSCAT data with the NSCAT-TC GMF, but with the rain rate set to zero in the MLE. Fig. 7 plots the wind speed along and across the spacecraft track through the center of cyclone. The correction of model function does make some improvement to the wind speed estimates, but the strength of the cyclone is still underestimated by up to about 20 m/s in comparison with the HRD analyses when the rain contamination is ignored.

With the SSM/I rain rate included in the wind retrievals, the along and across track profiles of QuikSCAT wind speed are illustrated in Fig. 8 for 25 km gridded resolution. The comparison with the HRD analyses is very well although the QuikSCAT wind speed is slightly lower near the eyewall. In addition, the 25 km gridded resolution is barely adequate to resolve the eye of the hurricane. The QuikSCAT wind retrievals at 12.5 km gridded resolution are compared with the HRD analyses in Fig. 9. There is a sharper wind gradient in the 12.5 km resolution wind than the 25 km resolution wind, the eye of the cyclone becomes more well-defined at a spatial gridded resolution of 12.5 km. In any case, the change of QuikSCAT wind speed along both cuts seems to correspond to the change of  $\sigma_0$  illustrated in Fig. 1.

The HRD wind analyses are provided on a latitude and longitude grid with a spatial resolution of about 2.7 km, which is

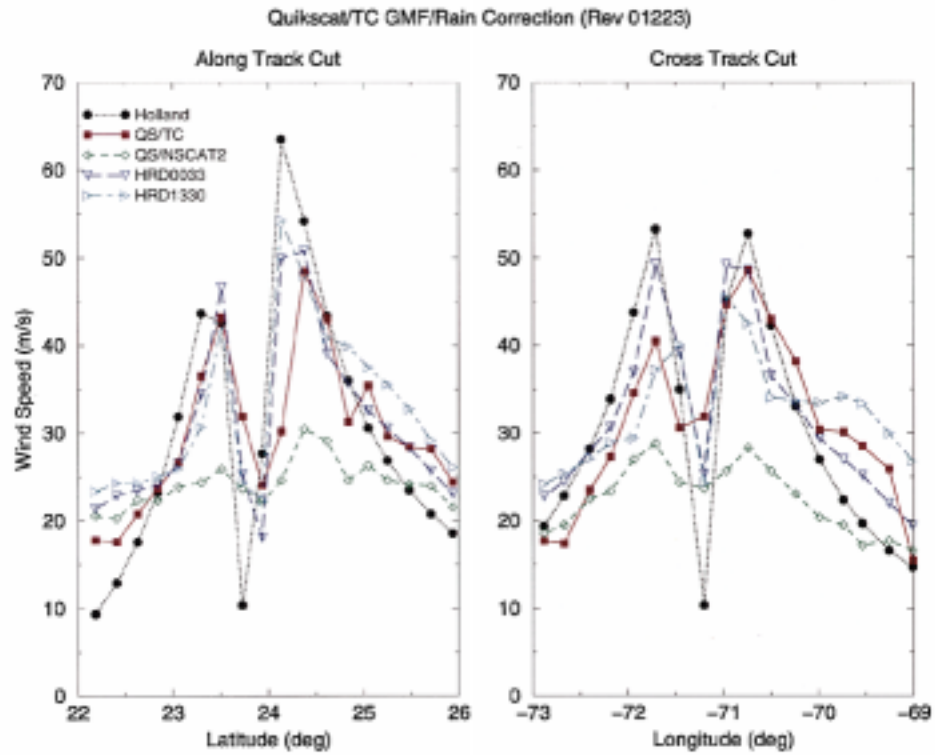


Fig. 8. Wind speed profiles of Hurricane Floyd on September 13, 1999. The left panel illustrates the along track cut through the center and the right panel illustrates the across-track cut. The wind vector cell resolution is 25 km. The QuikSCAT wind fields retrieved with the NSCAT2 GMF without rain correction (QS/NSCAT2) and the modified GMF with rain corrections (QS/TC) are illustrated. The Holland’s model wind is indicated by Holland and the HRD analyses at 00:33 UT and 13:30 UT are indicated by HRD0033 and HRD1330, respectively.

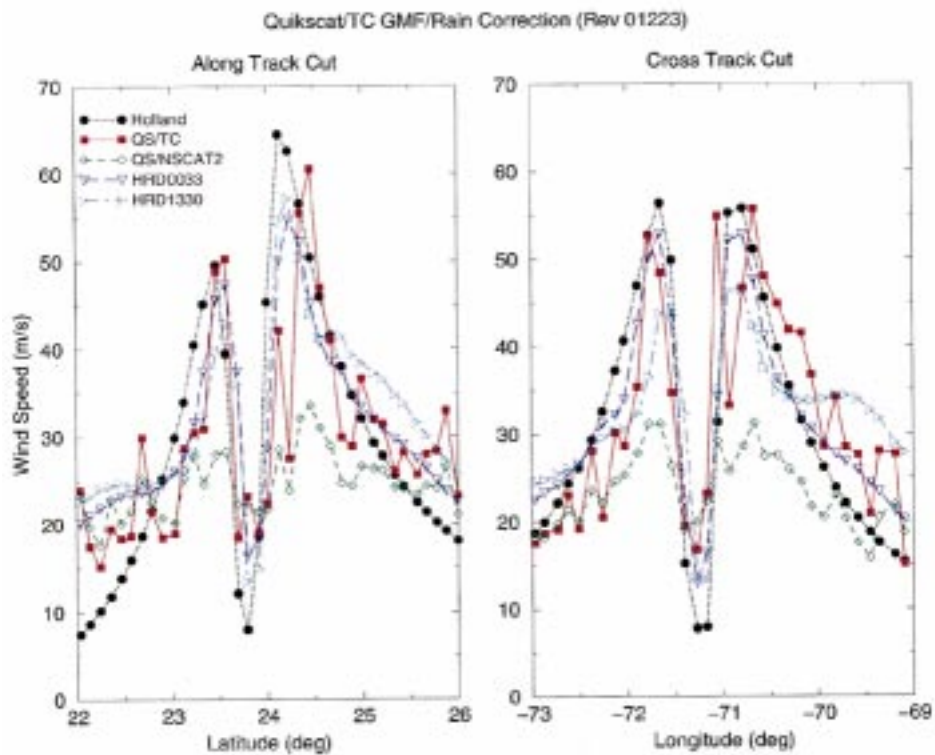


Fig. 9. Wind speed profiles of Hurricane Floyd on September 13, 1999. The left panel illustrates the along track cut through the center and the right panel illustrates the across-track cut. The wind vector cell resolution is 12.5 km. The QuikSCAT wind fields retrieved with the NSCAT2 GMF without rain correction (QS/NSCAT2) and the modified GMF with rain corrections (QS/TC) are illustrated. The Holland’s model wind is indicated by Holland and the HRD analyses at 00:33 UT and 13:30 UT are indicated by HRD0033 and HRD1330, respectively.

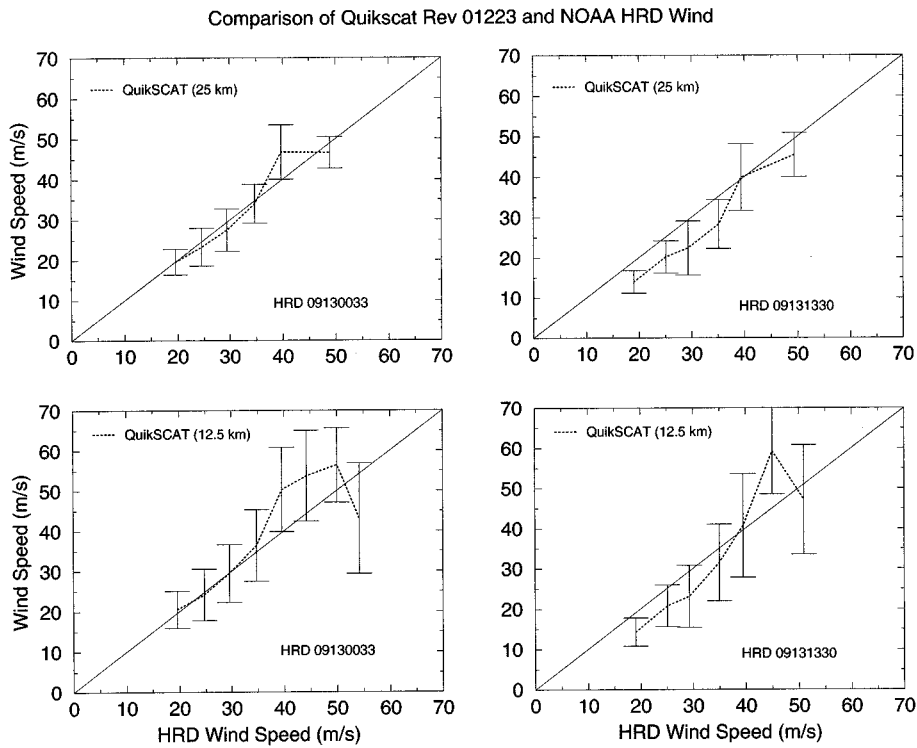


Fig. 10. Comparison of QuikSCAT wind speed estimates with the HRD wind analyses for Hurricane Floyd on September 13, 1999. The upper left panel compares the 25 km QuikSCAT wind with the HRD wind analyses at 00:33 UT and the upper right panel compares the 25 km QuikSCAT wind with the HRD wind analyses at 13:30 UT. The two lower panels compare the 12.5 km QuikSCAT wind with the HRD analyses. Lines with error bars indicate the QuikSCAT data.

significantly higher than the resolution of QuikSCAT  $\sigma_0$  and WVC. The HRD wind analysis on the grid point closest to the center of each QuikSCAT WVC is used for comparison with the QuikSCAT wind. We have neglected the effects of wind gradient in this comparison. In principle, the QuikSCAT winds represent some sort of spatial average over an area of about 50 to 100% larger than the size of the WVC, depending on the portion of collocated scatterometer  $\sigma_0$  cells falling outside of the WVC. It is not straightforward to quantify the resulting smoothing effect because the wind retrieval is a nonlinear optimization process and the smoothing effect depends on the size, shape and exact geometry of collocated  $\sigma_0$  cells with respect to the wind vector cell. For simplicity, we use Holland's model to estimate the effects of spatial averaging. We average Holland's hurricane winds with a  $25 \text{ km} \times 25 \text{ km}$  moving window for cyclones with various central pressure (920–970 mbar) and radius of maximum wind (20–40 km). We find that the spatial averaging has negligible effects (less than  $1 \text{ m} \cdot \text{s}^{-1}$  bias) for cells located more than 50 km off the eye, but can reduce the maximum wind speed by about 10 to 15% and can increase the wind in the eye by 5 to 20 m/s. The QuikSCAT wind velocity of about  $20 \text{ m} \cdot \text{s}^{-1}$  in the eye of Hurricane Floyd in Figs. 8 and 9, much higher than the forward motion of storm, reflects the wind gradient effects. Because we use Holland's model wind at the center of  $\sigma_0$  cell for the development of the NSCAT-TC model, part of the wind gradient effects has been included in the model function. The residual wind gradient effects on the reduction of maximum wind speed should be less than 10% in the QuikSCAT wind retrievals, which is small enough and will not alter our conclusion that including the rain rate in the model function brings

a positive impact on the QuikSCAT wind retrievals for tropical cyclones.

We make comparison of the QuikSCAT wind speed and HRD analyses at every QuikSCAT WVC location. The QuikSCAT wind retrievals are binned as a function of HRD wind speed with 5 m/s bin size. The average QuikSCAT wind speed is evaluated for each bin, so is the HRD wind speed. The standard deviation of the difference between QuikSCAT and HRD wind speeds is also evaluated. Four panels in Fig. 10 illustrate the QuikSCAT wind speed versus HRD wind speed for four cases: QuikSCAT wind retrievals at two resolutions in comparison with two HRD wind analyses. The QuikSCAT wind agrees very well with the HRD analyses at 00:33 UT, but not as well with the 13:30 UT analyses. The error bars indicate the standard deviation of wind speed differences in each wind speed bin. The standard deviation is about 3 m/s at near 20 m/s wind speeds at 25 km gridded resolution and increases with wind speed, reaching about 5–7 m/s at 50 m/s wind speed. Although the 12.5 km gridded wind has a better definition of the eye, its standard deviation is about two times that of the 25 km gridded QuikSCAT wind.

#### IV. SUMMARY

The radar measurements acquired for numerous tropical cyclones in 1999 by the NASA SeaWinds scatterometer were analyzed to improve the geophysical modeling of Ku-band ocean  $\sigma_0$ s and wind retrieval algorithm. The SeaWinds Scatterometer were deployed on the QuikSCAT spacecraft bus and has been operating since July 1999. We analyze the collocated QuikSCAT  $\sigma_0$  and SSM/I rain rates and propose an improved

QuikSCAT GMF for tropical cyclones. The surface wind fields for analysis were generated using the empirical Holland model. The QuikSCAT  $\sigma_0$ s were binned as a function of Hollnad's model wind speed and SSM/I rain rate. The average  $\sigma_0$  within each wind speed and rain rate bin was illustrated to indicate the wind speed and rain rate dependence. Our results suggest that the ocean  $\sigma_0$ s have a nonnegligible monotonic increasing dependence on wind speed from 20 to about 50 m/s for a large range of rain rate. The results were also used to improve the NSCAT2 GMF for extreme high wind speeds ( $> 20$  m/s). To account for the effects of rain, we include the rain rate as a parameter of the improved GMF.

We applied the improved GMF to the QuikSCAT wind retrievals for Hurricane Floyd at 12.5 km and 25 km gridded resolution. It is shown that the 12.5 km resolution can provide a better definition of the eye and can reduce the wind gradient errors, while the 25 km wind estimates have a smaller standard deviation. We demonstrate that the effects of rain have to be corrected to improve the wind retrievals. The inclusion of the SSM/I rain rates in the retrieval process greatly improve the retrieval accuracy. To assess the validity of our results, we make comparison of the QuikSCAT wind estimates and two wind analyses obtained from the NOAA HRD. The favorable comparison lends support to the possibility of obtaining useful wind fields from Ku-band spaceborne scatterometers.

We recommend three major areas for further study to improve the GMF and retrieval algorithms for tropical cyclones. In this article we did not address the wind direction dependence of  $\sigma_0$  for tropical cyclones. Our preliminary analysis based on the present collocated data set suggests that the wind direction variation of  $\sigma_0$  (about 1–2 dB) decreases with increasing wind speed and rain rate. However, the present data set is not large enough to make an accurate assessment of the wind direction modulations. The other area concerns the rain correction algorithm for the wind retrieval. Although the results of application to Hurricane Floyd is positive, we have to be cautious and do not want to extrapolate the results to other storms. We do not anticipate that the rain rate alone can enable an accurate wind retrieval for all types of storms because the precipitation is typically characterized by many parameters, including rain column height, vertical profile of rain and drop size distribution. We are in the process of applying our algorithms to a variety of TCs to evaluate the effectiveness and limitations of our algorithms for TCs at various stages. Finally, we recommend the use of more accurate operational analyses of tropical cyclones, such as those performed by the NOAA HRD, for the development of scatterometer GMF for extreme high winds. This will reduce the errors induced by the empirical Holland model.

#### ACKNOWLEDGMENT

We are grateful to the M. Freilich and B. Vanhoff of the Oregon State University and F. Wentz of Remote Sensing Systems for making the collocated SSM/I products available for this investigation. We appreciate the analyses of Hurricane Floyd provided by the NOAA Hurricane Research Division.

#### REFERENCES

- [1] M. A. Bender, R. J. Ross, R. E. Tuleya, and Y. Kurihara, "Improvements in tropical cyclone track and intensity forecasts using the GFDL initialization system," *Mon. Weath. Rev.*, vol. 121, pp. 2046–2061, 1993.
- [2] L. F. Bliven, P. W. Sobieski, and C. Craeye, "Rain generated ring-waves: Measurements and modeling for remote sensing," *Int. J. Remote Sens.*, vol. 18, no. 1, pp. 221–228, 1997.
- [3] C. Craeye, P. W. Sobieski, and L. F. Bliven, "Scattering by artificial wind and rain roughened water surfaces at oblique incidences," *Int. J. Remote Sens.*, vol. 18, no. 10, pp. 2241–2246, 1997.
- [4] J. Carswell, S. C. Carson, R. E. McIntosh, F. K. Li, G. Neumann, D. J. McLaughlin, J. C. Wilkerson, P. G. Black, and S. V. Nghiem, "Airborne scatterometers: Investigating ocean backscatter under low- and high-wind conditions," *Proc. IEEE*, vol. 82, pp. 1835–1860, Dec. 1994.
- [5] S. Dickinson and R. A. Brown, "A study of near-surface winds in marine cyclones using multiple satellite sensors," *J. Appl. Meteorol.*, vol. 35, pp. 769–781, June 1996.
- [6] W. J. Donnelly, J. R. Carswell, R. E. McIntosh, P. S. Chang, J. Wilkerson, F. Marks, and P. G. Black, "Revised ocean backscatter models at C and Ku-band under high wind conditions," *J. Geophys. Res.*, vol. 104, pp. 11 485–11 497, 1999.
- [7] M. H. Freilich and R. S. Dunbar, "Derivation of satellite wind model functions using operational surface wind analyses: An altimeter example," *J. Geophys. Res.*, vol. 98, pp. 14 633–14 649, 1993.
- [8] J. Graf, C. Sasaki, C. Winn, W. T. Liu, W. Tsai, M. Freilich, and D. Long, "NASA scatterometer experiment," *Asta Astron.*, vol. 43, pp. 397–407, 1998.
- [9] G. Holland, "An analytic model of the wind and pressure profiles in hurricanes," *Mon. Weath. Rev.*, vol. 108, pp. 1212–1218, 1980.
- [10] J. P. Hollinger, J. L. Peirce, and G. A. Poe, "SSM/I instrument evaluation," *IEEE Trans. Geosci. Remote Sensing*, vol. 28, pp. 781–790, September 1990.
- [11] C. Hsu and W. T. Liu, "Wind and pressure fields near tropical cyclone Oliver derived from scatterometer observations," *J. Geophys. Res.*, vol. 101, no. D12, pp. 17 021–17 027, July 1996.
- [12] C. S. Hsu, W. T. Liu, and M. G. Wurtele, "Impact of scatterometer winds on hydrologic forcing and convective heating through surface divergence," *Mon. Weath. Rev.*, vol. 125, pp. 1556–1576, July 1997.
- [13] W. L. Jones, V. J. Cardone, W. J. Pierson, J. Zec, L. P. Price, A. Cox, and W. B. Sylvester, "NSCAT high-resolution surface wind measurements in typhoon violet," *J. Geophys. Res.*, vol. 104, pp. 11 247–11 259, 1999.
- [14] W. T. Liu, H. Hu, and S. Yueh, "QuikSCAT and TRMM reveal the interplay between dynamic and hydrologic parameters in Hurricane Floyd," *EOS Trans.*, vol. 81, no. 23, pp. 253–257, June 2000.
- [15] F. M. Naderi, M. H. Freilich, and D. G. Long, "Spaceborne radar measurement of wind velocity over the ocean—An overview of the NSCAT scatterometer system," *Proc. IEEE*, vol. 79, pp. 850–866, June 1991.
- [16] M. D. Powell, "Evaluation of diagnostic marine boundary layer models applied to hurricanes," *Mon. Weath. Rev.*, vol. 108, pp. 758–766, 1980.
- [17] M. D. Powell, P. P. Dodge, and M. L. Black, "The landfall of Hurricane Hugo in the Carolinas," *Weath. Forecast.*, vol. 6, pp. 379–399, 1991.
- [18] M. D. Powell and S. H. Houston, "Hurricane Andrew's landfall in South Florida. Part II: Surface wind fields and potential real-time applications," *Weath. Forecast.*, vol. 11, pp. 329–349, 1996.
- [19] M. D. Powell, S. H. Houston, L. R. Amat, and N. Morisseau-Leroy, "The HRD real-time hurricane wind analysis system," *J. Wind Eng. Ind. Aerodynam.*, vol. 77–8, pp. 53–64, 1998.
- [20] M. D. Powell and S. H. Houston, "Surface wind fields of 1995 Hurricanes Erin, Opal, Luis, Marilyn and Roxanne at landfall," *Mon. Weath. Rev.*, vol. 126, pp. 1259–1273, 1998.
- [21] Y. Quilfen, B. Chapron, T. Elfouhaily, K. Katsaros, and J. Tournadre, "Observation of tropical cyclones by high-resolution scatterometry," *J. Geophys. Res.*, vol. 103, no. C4, pp. 7767–7786, Apr. 1998.
- [22] D. J. Shea and W. M. Gray, "The hurricane's inner core region, I: Symmetric and asymmetric structure," *J. Atmos. Sci.*, vol. 30, pp. 1544–1564, 1973.
- [23] A. Stoffelen and D. Anderson, "Scatterometer data interpretation: Estimation and validation of the transfer function CMOD4," *J. Geophys. Res.*, vol. 102, no. C3, pp. 5767–5780, Mar. 1997.
- [24] F. J. Wentz, M. H. Freilich, and D. K. Smith, "NSCAT-2 geophysical model function," in *Proc. 998 Fall AGU Meeting*, San Francisco, 1998.
- [25] F. J. Wentz and R. W. Spencer, "SSM/I rain retrievals within a unified all-weather ocean algorithm," *J. Atmos. Sci.*, vol. 55, no. 6, pp. 1613–1627, 1998.

- [26] I. R. Young, "An estimate of the geosat altimeter wind speed algorithm at high wind speeds," *J. Geophys. Res.*, vol. 98, pp. 20275–20285, Nov. 1993.
- [27] S. H. Yueh, R. West, F. Li, W.-Y. Tsai, and R. Lay, "Dual-polarized Ku-band backscatter signatures of hurricane ocean winds," *IEEE Geosci. Remote Sensing*, vol. 38, pp. 73–88, Jan. 2000.



**Simon H. Yueh** (M'92) received the S.B. and S.M. degrees from the Department of Electrical Engineering, National Taiwan University, Taiwan, R.O.C., in 1982 and 1984, respectively, and the Ph.D. degree in electrical engineering from the Massachusetts Institute of Technology, Cambridge, in 1991.

He was a Postdoctoral Research Associate with MIT from February to August, 1991. He developed various techniques for the calibration of polarimetric radars and theoretical models for the remote sensing of rough surfaces and vegetation. In 1991, he joined the Radar Science and Engineering Section, Jet Propulsion Laboratory (JPL), Pasadena, CA. At JPL, he has been working on advanced active and passive microwave techniques for ocean surface remote sensing. He has been the Principal Investigator and Co-Investigator of numerous NASA and NPOESS projects. He has authored four book chapters and published 43 refereed articles. His current fields of interest include techniques and instrument developments for microwave remote sensing of soil moisture, ocean surface salinity, ocean winds, and polar ice. He is a member of the Salinity Sea Ice Working Group.

Dr. Yueh was the recipient of the 1996 NASA Scatterometer Group Achievement Award. He received the 1995 IEEE GRSS Transaction Prize Paper award for a paper on polarimetric radiometry. He also received the 1998 JPL Director Lew Allen Award for Excellence in recognition of his pioneering research of passive microwave polarimetric remote sensing to Earth surface investigations. His paper on the spaceborne scatterometer applications for hurricane wind retrieval was awarded the best symposium paper in the International Geoscience and Remote Sensing Symposium 2000.



**Bryan W. Stiles** (S'94–M'97) received the B.S. degree in electrical engineering from the University of Tennessee, Knoxville, in 1992 and the Ph.D. degree from the University of Texas, Austin, in 1997, where his doctoral dissertation proved the universal approximation capability of certain dynamic artificial neural networks. In June 1997, he became a member of Technical Staff, Jet Propulsion Laboratory, Pasadena, CA, where he has simulated the behavior of spaceborne scatterometers (NSCAT and SeaWinds) as well as analyzed the data returned

from these instruments. He is interested in statistical techniques for determining and visualizing relationships between remote sensor data and geophysical phenomena.

**Wu-Yang Tsai** received the Ph.D. degree in theoretical physics from Harvard University, Cambridge, MA, in 1971.

He has performed research in high energy physics, classical and quantum electrodynamics, electromagnetic scattering, propagation and radiation, high-density plasma fusion, high-altitude nuclear explosion phenomenology, radiative heat transfer, synthetic aperture radar (SAR), and currently, on all aspects of scatterometer design, algorithm development, and science applications. He co-authored the graduate level text book *Classical Electrodynamics* with Julian Schwinger et. al, and is currently a Principal Engineer with the Jet Propulsion Laboratory, Pasadena, CA, and is the Project Engineer of SeaWinds on QuikSCAT (QSCAT), SeaWinds on ADEOS-2 (SeaWinds) and advanced scatterometer projects. He is also the Group Supervisor of the Scatterometer System Engineering Group.



**Hua Hu** received the Ph.D. degree in geophysics in 1994.

She is a Senior Member of Technical Staff in the Ocean Sciences Element, Jet Propulsion Laboratory (JPL), California Institute of Technology, Pasadena, CA. She then joined JPL as a Postdoctoral Research Associate. She has an extensive background in field experiments and has participated in many successful science campaigns involving aircraft, balloon, and rocket flights for studying atmospheric and space sciences. She has been working on deriving scientific

applications from remote sensing instruments. Her current research interests include hydrologic cycle, air-sea interaction, and tropical cyclone development. She has 15 refereed journal publications.

Dr. Hu received a NASA Group Achievement Award.



**W. Timothy Liu** received the Ph.D. degree in atmospheric sciences from the University of Washington, Seattle, in 1978.

He has been a Principal Investigator on studies concerning ocean-atmosphere interaction and satellite oceanography since he joined the Jet Propulsion Laboratory, California Institute of Technology, Pasadena, CA, in 1979. He has been the Leader of the Air-Sea Interaction and Climate Team, supervising a team of meteorologists and oceanographers since 1989. He has been the Project

Scientist of NASA space missions, NSCAT since 1992, and QuikSCAT since 1997. He was a member of various working groups of the World Climate Research Program as well.

Dr. Liu is a Fellow of the American Meteorological Society and received the NASA Medal for Exceptional Scientific Achievement for his pioneering work in ocean surface heat flux in 1990 and the NASA Exceptional Achievement Medal in leading the NSCAT Science Team in air-sea interaction studies in 1998. He has received numerous NASA Certificates of Recognition for the innovative work and NASA Group Achievement Awards related to his work in NASA flight missions. He was selected as principal investigators of a number of NASA flight missions, including NSCAT, Topex/Poseidon, TRMM and EOS Interdisciplinary Sciences. He has served on numerous science working groups and advisory panels of NASA, including the Advisory Committee of the NASA Earth Science Division.